

Published in final edited form as:

Fungal Genet Biol. 2009 ; 46(0): 496–505. doi:10.1016/j.fgb.2009.03.003.

Structural and functional properties of the *Trichosporon asahii* glucuronoxylomannan

Fernanda L. Fonseca^a, Susana Frases^b, Arturo Casadevall^{b,c}, Olga Fischman-Gompertz^d, Leonardo Nimrichter^a, and Marcio L. Rodrigues^{a,*}

^aLaboratório de Estudos Integrados em Bioquímica Microbiana, Instituto de Microbiologia Professor Paulo de Góes, Universidade Federal do Rio de Janeiro, Avenida Carlos Chagas Filho, 373, Cidade Universitária CCS, Bloco I, Rio de Janeiro – RJ 21941-902, Brazil

^bDepartment of Microbiology and Immunology, Albert Einstein College of Medicine, 1300 Morris Park Ave. Bronx, NY 10461, USA

^cDivision of Infectious Diseases of the Department of Medicine, Albert Einstein College of Medicine, 1300 Morris Park Ave. Bronx, NY 10461, USA

^dDisciplina de Biologia Celular, Universidade Federal de São Paulo, São Paulo, SP 04023-062, Brazil

Abstract

The virulence attributes of *Trichosporon asahii* are virtually unknown, despite its growing relevance as causative agent of superficial and invasive diseases in humans. Glucuronoxylomannan (GXM) is a well described virulence factor of pathogenic species in the *Cryptococcus* genus. GXM is also produced by species of the *Trichosporon* genus, and both polysaccharides share antigenic determinants, but unlike cryptococcal GXM, relatively little work has been done on trichosporal GXMs. In this study, we analyzed structural and functional aspects of GXM produced by *T. asahii* and compared them to the properties of the cryptococcal polysaccharide. Trichosporal and cryptococcal GXM shared antigenic reactivity, but the former polysaccharide had smaller effective diameter and negative charge. GXM anchoring to the cell wall was perturbed by dimethylsulfoxide and required interactions of chitin-derived oligomers with the polysaccharide. GXM from *T. asahii* supernatants are incorporated by acapsular mutants of *Cryptococcus neoformans*, which renders these cells more resistant to phagocytosis by mouse macrophages. In summary, our results establish that despite similarities in cell wall anchoring, antigenic and antiphagocytic properties, trichosporal and cryptococcal GXMs manifest major structural differences that may directly affect polysaccharide assembly at the fungal surface.

Keywords

Trichosporon; Glucuronoxylomannan; Phagocytosis

1. Introduction

Species belonging to the *Trichosporon* genus include basidiomycetes yeast found on human skin (Antachopoulos et al., 2007; Pfaller and Diekema, 2004). *Trichosporon* species have been reported to be the most common cause of non-candidal yeast-associated disease in patients with hematological malignancies, a condition that is associated with mortality rates in excess of 80% (Pfaller and Diekema, 2004). Up to 88% of deep-seated *Trichosporon* infections are caused by *Trichosporon asahii*, which is resistant to most of the clinically used antifungal drugs (Pfaller and Diekema, 2004). Clinical treatment failures with amphotericin B, fluconazole, and combinations of the two have been reported in human cases of trichosporonosis (reviewed in Pfaller and Diekema (2004)). Although *T. asahii* is an emerging pathogen resistant to most currently available antifungal therapies, its virulence factors and pathogenic mechanisms are largely unknown.

Glucuronoxylomannan (GXM) is a cell wall-associated and secreted polysaccharide produced by species of the genus *Trichosporon* (Ichikawa et al., 2001; Karashima et al., 2002) and *Cryptococcus* (reviewed in Bose et al. (2003)). In *T. asahii*, GXM building blocks consist of an α 1,3-D-mannan-like hexasaccharide substituted with one β 1,2-glucopyranosyluronic acid residue and six β -D-xylopyranosyl units (Fig. 1 and Ichikawa et al., 2001). Xylosylation includes O-2, O-4 and O-6 substitutions of the mannose residues.

In contrast to *Trichosporon* GXM, the structure and function of cryptococcal GXMs have been widely studied. In *Cryptococcus* spp., GXM is an extracellular/cell associated capsular polysaccharide that down modulates the immune response of infected individuals (Monari et al., 2006). Cryptococcal GXM is thought to have protean functions in virulence including protecting yeast cells against phagocytosis and oxidative burst (Kozel and Gotschlich, 1982; Zaragoza et al., 2008), impairing immune function through various mechanisms (Vecchiarelli, 2007) and promoting intracellular survival (Feldmesser et al., 2001). Cryptococcal GXM consists of a high-molecular mass polysaccharide (McFadden et al., 2006) that is synthesized in the Golgi apparatus and then packaged into vesicles destined to be released to the extracellular space (Panepinto et al., 2009; Rodrigues et al., 2007, 2008b; Yoneda and Doering, 2006). GXM is connected to cell wall through linkages to structural polysaccharides (Reese and Doering, 2003; Reese et al., 2007; Rodrigues et al., 2008a) and finally used for distal, cation-mediated capsular enlargement (Frasces et al., 2009; Nimrichter et al., 2007; Zaragoza et al., 2006).

Although several structural aspects of *T. asahii* GXM have been described (Ichikawa et al., 2001), the functions of this polysaccharide for physiology and pathogenesis of *Trichosporon* spp. are virtually unknown. A comparative study revealed that *Cryptococcus* and *Trichosporon* isolates, which both express surface GXM, were less efficiently ingested by phagocytes than *Candida* strains (Lyman and Walsh, 1994). However, a direct role of GXM in protection of *Trichosporon* cells against phagocytosis was not demonstrated. A role for GXM in the pathogenicity of *T. asahii* was suggested by the observation that successive steps of inoculation and recovery of *T. asahii* from mice resulted in an increased release of the polysaccharide in culture supernatants (Karashima et al., 2002). Serological similarities of *Cryptococcus* and *Trichosporon* GXMs have also been reported. An antibody to

cryptococcal capsular polysaccharides was demonstrated to cross-react with cell wall components of a *Trichosporon* isolate (Melcher et al., 1991). The mechanisms by which the *Trichosporon* GXM interacts with other cell wall components, however, are not known.

In this study, we analyzed several properties of GXM from *T. asahii*, including structural aspects, antibody reactivity, self-aggregation, surface expression, extracellular release, cell wall connections and antiphagocytic properties. Our results revealed both similarities and differences among cryptococcal and trichosporal GXMs. The potential impact of these findings on fungal pathogenesis and surface architecture is discussed.

2. Methods

2.1. Fungal strains

The *T. asahii* isolates used in this study included the standard strain CBS 2479 and the clinical isolate EPM21-05. The *Cryptococcus neoformans* isolates were the Brazilian clinical isolates HEC3393 and T₁444, which are serotype A strains expressing small and large capsules, respectively (Barbosa et al., 2006), the standard strain H99 (serotype A) and the acapsular mutant Cap67. Stock cultures were maintained in Sabouraud dextrose agar under mineral oil and kept at 4 °C. Yeast cells were grown in a chemically defined medium (pH 5.5) composed of glucose (15 mM), MgSO₄ (10 mM), KH₂PO₄ (29.4 mM), glycine (13 mM) and thiamine-HCl (3 µM) for 4 days (*T. asahii*), at 25 °C (*C. neoformans* and *T. asahii*) or 37 °C (*T. asahii*).

2.2. GXM purification

The basic protocol for polysaccharide purification was recently described by our group (Nimrichter et al., 2007). Fungal cells were cultivated with shaking for 4 days at room temperature in the minimal medium described above and separated from culture supernatants by centrifugation at 4000g (15 min, 4 °C). For both *C. neoformans* and *T. asahii*, cell densities were in the range of 2–8 × 10⁷ cells/ml at day four of cultivation. The supernatant fluids were collected by centrifugation and again centrifuged at 15,000g (15 min, 4 °C), to remove smaller debris. The pellets were discarded and the resulting supernatant was concentrated approximately 20-fold using an Amicon (Millipore, Danvers, MA) ultrafiltration cell (cutoff = 100 kDa, total capacity of 200 ml) with stirring and Biomax polyethersulfone ultrafiltration discs (63.5 mm). Nitrogen (N₂) stream was used as the pressure gas. After supernatant concentration, the fluid phase was discarded, and the viscous layer was collected with a cell scraper and transferred to graduated plastic tubes for measurement of gel volumes. The procedure was repeated at least three times to ascertain average volumes.

2.3. Monosaccharide analysis

Carbohydrate composition analysis of the jellified GXM fractions from *T. asahii* and *C. neoformans* was performed by gas chromatography/mass spectrometry (GC/MS) analysis of the per-*O*-trimethylsilyl (TMS) derivatized monosaccharides from the polysaccharide films (Merkle and Poppe, 1994). Polysaccharide samples (0.3 mg) were methanolized in methanol/1 M HCl at 80 °C (18–22 h) for further per-*O*-trimethylsilylation with Tri-Sil

(Pierce) at 80 °C (0.5 h). GC/MS analysis of the volatile per-*O*-TMS derivatives was performed on an HP 5890 gas chromatograph interfaced to a 5970 MSD mass spectrometer, using a Supelco DB-1 fused silica capillary column (30 m × 0.25 mm ID). Arabinose, rhamnose, fucose, xylose, glucuronic acid, galacturonic acid, mannose, galactose, glucose, mannitol, dulcitol and sorbitol were used as monosaccharide standards.

2.4. Zeta potential determinations in extracellular GXM fractions

Zeta potential (ξ), particle mobility and shift frequency of polysaccharide samples were calculated in a Zeta potential analyzer (ZetaPlus, Brookhaven Instruments Corp., Holtsville, NY). Polysaccharide samples were dissolved in water to generate 1 mg/ml solutions. Values of ξ were calculated using the equation $\xi = (4\pi\eta m)/D$, where D is the dielectric constant of the medium, η is the viscosity and m is the electrophoretic mobility of the particle.

2.5. GXM effective diameter

Effective diameter and size distribution of GXM preparations were measured by quasi-elastic light scattering in a 90Plus/BI-MAS Multi Angle Particle Sizing analyzer (Brookhaven Instruments Corp., Holtsville, NY), according with the method described by our group (Frasces et al., 2009). GXM solutions were all used at 1 mg/ml. The autocorrelation function $C(t)$, where $C(t) = Ae^{2\Gamma t} + B$, was used to process the fluctuating signal, originating from the random motion of particles in a liquid phase and the associated alterations in the intensity of the scattered light over time. In this equation, t is the time delay, A is an optical constant determined by the instrument design and Γ is related to the relaxation of the fluctuations by $\Gamma = Dq^2$. The value of q is calculated from the scattering angle θ , the wavelength of the laser light λ_0 and the index of refraction n of the suspended liquid, according to the equation $q = (2\pi n/\lambda_0) 2\text{Sin}(\theta/2)$. Particle size is related to the translational diffusion coefficient (D) for shapes including spheres, ellipsoids, cylinders and random coils. Assuming the spherical form as the most useful in the greatest number of cases, the equation $D = (K_B T)/(3\pi\eta(t)d)$, where K_B is Boltzmann's constant (1.38054×10^{-16} ergs/deg), T is the temperature in K (30 °C), $\eta(t)$ is the viscosity of the liquid in which the particles are moving and d is the particle diameter, was used. All GXM samples were analyzed under the same conditions. Multimodal size distribution analysis of polysaccharides was calculated from the values of intensity weighted sizes obtained from the non-negatively constrained least squared (NNLS) algorithm.

2.6. Enzyme-linked immunosorbent assays (ELISA) using fungal polysaccharides

The reactivity of *T. asahii* GXM with a monoclonal antibody (mAb) to the cryptococcal polysaccharide was determined by ELISA, using modifications of a previously described protocol for GXM detection (Casadevall et al., 1992). 96-Well polystyrene plates were coated with 5 µg/ml solutions of *T. asahii* (isolate CBS2479) GXM and incubated for 1 h at 37 °C. Alternatively, the plates were coated with a solution of *Saccharomyces cerevisiae* mannan (negative control) at the same concentration. Polysaccharide concentration was ascertained using the method described by Dubois (Dubois et al., 1951). After removal of unbound polysaccharide, the plates were blocked with 1% bovine serum albumin, followed by addition of a solution of mAb 18B7, an IgG1 with affinity for GXM of different

serotypes (Casadevall et al., 1998). After incubation for 1 h at 37 °C, the plates were washed five times with tris-buffered saline (TBS) supplemented with 0.1% Tween 20, followed by incubation with an alkaline phosphatase-conjugated goat anti-mouse IgG1 for 1 h. Reactions were developed after the addition of *p*-nitrophenyl phosphate disodium hexahydrate, followed by measuring absorbance at 405 nm with a microplate reader (TP-reader, Thermo Plate). Antibody concentration in this assay corresponded to 1 µg/ml.

2.7. GXM release after treatment of *T. asahii* with chitinase

After extensive washing with PBS, yeast cells (10^6) were suspended in 100 µl of 0.01 M phosphate buffer (pH 6.0) containing chitinase (100 µg/ml, Sigma, purified from *Streptomyces griseus*), followed by incubation at 37 °C for 12 h. The cell suspensions were incubated overnight at 37 °C and centrifuged at 4000 rpm for cell removal. Controls included cells treated in buffer containing no enzyme. The presence of GXM in supernatants was determined by capture ELISA, as described previously (Casadevall et al., 1992). Control or chitinase-treated cells were analyzed by fluorescence microscopy as described further in this section.

2.8. DMSO extraction

The protocol used for GXM extraction from *T. asahii* was based on studies developed with *C. neoformans* (Bryan et al., 2005). Yeast cells (1.5×10^9) were suspended in 15 ml DMSO. The cells were then incubated for 30 min at room temperature with shaking and the supernatants were collected. Pellets were resuspended in 15 ml DMSO and again incubated for 30 min. The cells were extensively washed in PBS and prepared for immunofluorescence with mAb 18B7 as described below.

2.9. Fluorescence microscopy

The different systems tested in this assay included control cells of *C. neoformans* or *T. asahii*, as well as fungi treated with DMSO or chitinase. Yeast cells (10^6) were suspended in 4% paraformaldehyde cacodylate buffer (0.1 M, pH 7.2) and incubated for 30 min at room temperature. Fixed yeast cells were washed twice in PBS and incubated in 1% bovine serum albumin in PBS (PBS-BSA) for 1 h. For GXM staining, blocked cells were incubated with mAb 18B7 (1 µg/ml) for 1 h at room temperature, followed by a fluorescein isothiocyanate (FITC) labeled goat anti-mouse IgG (Fc specific) antibody (Sigma). For staining with fluorescent wheat germ agglutinin (WGA), yeast cells were suspended in 100 µl of a 5 µg/ml solution of the Alexa Fluor 594 conjugate of the lectin (Molecular Probes) and incubated for 30 min at 37 °C. After incubation with the fluorescent probes, the cells were washed with PBS and observed under fluorescence microscopy. Alternatively, WGA-stained cells were sequentially incubated with mAb 18B7 and secondary antibodies as described above. To eliminate the possibility that the fluorescence pattern was derived from a specific sequential use of reagents, the order of the reagents was changed and the results were the same (data not shown). Images were obtained after placing yeast cell suspensions in mounting medium (50% glycerol and 50 mM *N*-propyl gallate in PBS) over glass slides followed by observation under an Axioplan 2 (Zeiss, Germany) fluorescence microscope. Images were acquired using a Color View SX digital camera and processed with the software system

analysis (Soft Image System). Images were finally processed using ImageJ software (provided by NIH, <http://rsb.info.nih.gov/ij/>).

2.10. Flow cytometry analysis

Yeast cells of *T. asahii* or *C. neoformans* were washed in PBS and fixed in 4% paraformaldehyde cacodylate buffer 0.1 M, pH 7.2 for 1 h at room temperature. Fixed yeast cells were washed again in PBS and incubated in 1% bovine serum albumin in PBS (PBS–BSA) for 1 h at room temperature. The cells were then washed twice in PBS and sequentially incubated with mAb 18B7 (1 µg/ml) and fluorescein isothiocyanate (FITC) labeled anti-mouse IgG (1 µg/ml) for 1 h, at room temperature. Yeasts were again washed and 5000 cells were analyzed in a FACS Calibur (BD Biosciences, San Jose, CA) flow cytometer. Data were processed with CellQuest (BD Biosciences) or WinMDI (Salk Flow Cytometry) software. Control cells, in which mAb 18B7 was replaced by isotype-matched irrelevant antibodies, were analyzed first.

2.11. GXM binding by acapsular cells

Acapsular *C. neoformans* cells (strain Cap67, 10⁶ cells) were suspended in 100 µl of culture supernatants (4 day cultures) from *C. neoformans* (H99 strain) or *T. asahii* (isolates CBS 2479 or EPM21-05). GXM in supernatants was normalized to 10 µg/ml. The suspension was incubated for 12 h at 25 °C and extensively washed with PBS. Control systems consisted of Cap67 cells incubated with sterile medium. For immunofluorescence with mAb 18B7, the cells were fixed with 4% paraformaldehyde and prepared as described above. For phagocytosis assays, yeast suspensions were prepared and incubated with macrophages, as described below.

2.12. Phagocytosis

The murine macrophage cell line RAW 264.7 (American Type Culture Collection, Rockville, MD) was grown to confluence in 25 cm² culture flasks containing Dulbecco's modified Eagle's medium (DMEM) supplemented with 10% fetal bovine serum (FBS), at 37 °C in a 5% CO₂ atmosphere. For interaction with yeast cells, the macrophages were cultivated over sterile glass slides placed onto the wells of a 24-well plate, in the same conditions described above. Yeast suspensions were prepared in DMEM, to generate a ratio of 10 yeasts per macrophage-like cell. Interactions between fungal and host cells occurred at 37 °C at a 5% CO₂ atmosphere for 4 h. After removal of non-adherent fungi by washing, the cells were fixed with Bouin's solution and stained with Giemsa. In each system, 200 macrophages were counted and the index of association between *C. neoformans* and host cells was considered as the total number of yeasts per 100 phagocytes. All experiments were performed in triplicate sets and statistically analyzed by using Student's *t*-test.

3. Results

3.1. Isolation of Trichosporon GXM by ultrafiltration

GXM isolation by ultrafiltration is an efficient method for purification of the polysaccharide from *C. neoformans* (Nimrichter et al., 2007). Since *T. asahii* also releases GXM (Karashima et al., 2002), we evaluated whether the protocol previously used for isolation of

GXM in *C. neoformans* supernatants was suitable for the recovery of trichosporal GXM. Gel formation with cryptococcal supernatants (strain T₁444) was observed when 400 ml fungal cultures containing at least 3×10^{10} cells were concentrated 20-fold in the ultrafiltration cell. Under the same conditions, gel formation was not observed after filtration of supernatants from *T. asahii* (data not shown). We therefore gradually increased culture volumes and kept constant the final volume of concentrated supernatants, generating, therefore, progressively more concentrated supernatants. Gel formation deriving from trichosporal supernatants were only observed after the culture fluids at a similar cell density were 300-fold concentrated. Carbohydrate determinations according to the method of Dubois (Dubois et al., 1951) revealed that GXM concentration in cryptococcal polysaccharide gels was approximately 13-fold higher than in the *Trichosporon* fractions. Therefore, we concluded that formation of GXM films is more efficient in *C. neoformans* than in *T. asahii*. This analysis was repeated at least three times showing similar profiles of GXM aggregation. A representative experiment is shown in Table 1.

3.2. Structural and serologic properties of GXM

The components of GXM, mannose, xylose and glucuronic acid, were detected in *T. asahii* ultrafiltration fractions by GC-MS (Fig. 2A). Glucose and galactose, which were already described as GXM contaminants in fractions purified by ultrafiltration (Frases et al., 2008), were also detected in the *T. asahii* preparations. The *C. neoformans* (strain T₁444) ultrafiltration fraction was analyzed under the same conditions, revealing a similar compositional profile. Therefore, based on the currently presented data and the previous literature (Frases et al., 2008; Nimrichter et al., 2007), the *T. asahii* fraction obtained by ultrafiltration is likely to correspond to GXM, since it is a partially purified polysaccharide preparation containing the GXM building units. It is noteworthy to mention that the content of glucuronic acid in the samples described above is possibly underestimated, since this acidic sugar usually gives, after methanolysis and TMS-derivatization, minor peaks on the chromatogram that may be superposed on the peaks of galactose and glucose (Fenselau and Johnson, 1980), affecting its quantitative analysis.

Antibodies to cryptococcal GXM were previously demonstrated to cross-react with *Trichosporon* polysaccharides (Melcher et al., 1991). In addition, mAb 18B7 reacts with different GXM structures (Casadevall et al., 1998). The mAb to the cryptococcal polysaccharide, indeed, reacted with the *T. asahii* GXM (Fig. 2B). This result is consistent with the fact that *T. asahii* and *C. neoformans* GXMs share common domains (Fig. 1).

The size of extracellular GXM fibers from *T. asahii* was analyzed by dynamic light scattering. GXM fibers were in the range of 100–2700 nm (Fig. 3), with an average effective diameter corresponding to 814.6 ± 35.3 nm. Similar analyses were performed with ultrafiltration fractions from strains T₁444 and HEC3393 of *C. neoformans*, which had effective diameter values corresponding to 2635 ± 95.6 and 1342.7 ± 29.4 , respectively. Median values corresponded to 770 nm for *T. asahii*, 2557.85 nm for the cryptococcal strain T₁444, and 1333.5 nm for the HEC3393 isolate of *C. neoformans*. Therefore, the GXM fibers secreted by *T. asahii* are smaller than those produced by *C. neoformans* cells. The analysis of the electro-negativity of different GXM fractions revealed Zeta potential values

of -29.17 ± 0.76 mV for *T. asahii* and -38.15 ± 0.41 mV for *C. neoformans* (strain T₁₄₄₄). The higher Zeta potential value obtained for the *C. neoformans* GXM is consistent with its increased content of glucuronic acid, in comparison with the *Trichosporon* polysaccharide (Fig. 2A).

The expression of surface GXM in *T. asahii* and *C. neoformans* was also compared by fluorescence-based methods (Fig. 4). Controls consisting of acapsular *C. neoformans* cells (strain cap67) were prepared for immunofluorescence following the same steps used for the analysis of *T. asahii* and encapsulated *C. neoformans* cells. In microscopic analysis, the fluorescence levels for the controls were similar to those observed when the step of incubation with the antibody to GXM was omitted during preparation of *T. asahii* and encapsulated *C. neoformans* cells (data not shown). In flow cytometry assays, the maximum percentage of fluorescent acapsular cells corresponded to 3% (not shown).

Microscopic observations of *T. asahii* revealed cell populations consisting mostly of round and ovoid yeast cells in the range of 3–7 μ m (Figs. 4 and 5). The presence of differentiating forms resembling mycelial cells was observed occasionally. In fluorescence microscopy, images in all systems were acquired under the same conditions. Therefore, the results suggested that antibody reactivity with the *C. neoformans* surface was more intense than that observed in any other system. Interestingly, in one of the *T. asahii* isolates, fluorescent antibody–polysaccharide reactions were less intensive when the fungus was cultivated at 37 °C than when the cells were grown at 25 °C. The visual differences observed under fluorescence microscopy led us to quantify the reactivity of mAb 18B7 with fungal cells by flow cytometry.

As expected, the two different *C. neoformans* isolates (strains T₁₄₄₄ and HEC3393) were efficiently recognized by the antibody (Fig. 4). In both strains, more than 90% of the population reacted with mAb 18B7. In contrast, the maximum percentage of fluorescent-positive cells in *T. asahii* was in the range of 29% (strain EPM21-05). As suggested by fluorescence microscopy, GXM expression in the EPM21-05 isolate was down modulated at 37 °C. In addition to a higher percentage of fluorescent cells, the intensity of the fluorescent reactions with cryptococcal cells was much higher than those with the *T. asahii* isolates.

3.3. GXM anchoring to the cell wall of *T. asahii*

In *C. neoformans*, oligosaccharides composed of *N*-acetylglucosamine (chitoooligomers) are involved in GXM anchoring to the cell wall (Rodrigues et al., 2008a). To analyze GXM-cell wall connections in *T. asahii*, we evaluated the reactivity of fungal cells with the lectin WGA, which recognizes *N*-acetylglucosamine-containing structures that connect the cell wall to the capsule of *C. neoformans* (Rodrigues et al., 2008a). The profile of WGA staining in *T. asahii* (Fig. 5A) was very similar to that observed previously for *C. neoformans* (Rodrigues et al., 2008a), which includes a strong reactivity with bud-associated structures. Treatment of *T. asahii* with chitinase resulted in the release of surface GXM, as demonstrated by ELISA of extracellular fractions (Fig. 5B) and immunofluorescence of fungal cells (Fig. 5C). In control cells, WGA binding was concentrated at budding sites. Chitinase treatment, however, modified the punctate profile of lectin binding to the cell surface to a diffuse pattern, resulting in indiscriminate staining of the cell wall. Similar

observations were described for *C. neoformans* (Rodrigues et al., 2008a). Differentiating *T. asahii* cells were also recognized by the antibody to GXM and by WGA, suggesting that polysaccharide anchoring in mycelial forms follows the same pattern observed for yeast cells. GXM anchoring to the cell wall was demonstrated to be sensitive to DMSO treatment in *C. neoformans* (Bryan et al., 2005). In *T. asahii*, DMSO-treated cells were not recognized by the anti-GXM antibody (Fig. 6). We interpreted this result as a consequence of the release of surface GXM rather than loss of reactivity with the antibody, since supernatant fractions of DMSO treatments were still recognized by mAb 18B7 in ELISA after extensive dialysis (data not shown).

C. neoformans acapsular mutants that have defective GXM secretion are able to incorporate exogenously added GXM into the cell surface (Reese and Doering, 2003). The similarities in cell wall anchoring shared by cryptococcal and *Trichosporon* GXMs led us to evaluate the whether acapsular mutant of *C. neoformans* would incorporate heterologous GXM. The *C. neoformans* acapsular mutant became reactive with mAb 18B7 after incubation in the presence of different *T. asahii* culture supernatants (Fig. 7). The fact that the *C. neoformans* mutant became coated with *T. asahii* GXM allowed us to design an experimental system to evaluate whether the *Trichosporon* polysaccharide is antiphagocytic, as previously hypothesized in the literature (Lyman and Walsh, 1994).

3.4. The *T. asahii* GXM has antiphagocytic properties

After incubation with supernatants from an encapsulated strain of *C. neoformans* (strain H99), culture fluids of two *T. asahii* isolates or sterile medium, the cryptococcal acapsular mutant Cap67 was incubated with mouse macrophages for phagocytosis determination (Fig. 8). Yeast cells containing no detectable surface GXM were readily phagocytized by the macrophages. GXM-coated cells, however, were much more resistant to phagocytosis. The phagocytic index for polysaccharide-coated yeast cells were around six-fold smaller than for cells containing no GXM. Acapsular mutants coated with GXM from *C. neoformans* or *T. asahii* were similarly resistant to phagocytosis.

4. Discussion

Structural and serological analyses have shown similarities and differences between the polysaccharides from *Cryptococcus* and *Trichosporon* (Ichikawa et al., 2001; Melcher et al., 1991). Depending on the species and related serotype, the building motifs of the cryptococcal GXM vary in complexity (Cherniak et al., 1998). The repeating motif of the *Trichosporon* GXM appears to be even more complex (Ichikawa et al., 2001). A comparison with the *Cryptococcus* motifs reveals that the *Trichosporon* polysaccharide manifested more variability in its structural features. These differences include a higher degree of xylosylation that forms disaccharyl branches, which are absent in *Cryptococcus* and different linkages connecting xylosyl units to the mannose backbone (Ichikawa et al., 2001). However, polysaccharides from both genera also share similar motifs, as the one highlighted in Fig. 1. Structural analysis of GXM fractions obtained from *T. asahii* and *C. neoformans* by ultrafiltration also revealed similarities in monosaccharide composition. The relative content of glucuronic acid in the *T. asahii* GXM, however, was approximately twofold

smaller than in the cryptococcal polysaccharide, which probably accounts for its reduced value of Zeta potential. The *Trichosporon* GXM also showed a smaller effective diameter.

In *C. neoformans*, the ability of GXM to self-aggregate was determined based on the efficacy of formation of polysaccharide-containing gels after concentration of culture supernatants (Nimrichter et al., 2007). GXM self-aggregation, which requires the negative charges of glucuronic acid units (Nimrichter et al., 2007), was demonstrated to influence capsule assembly and enlargement in this species (Frasés et al., 2008; Nimrichter et al., 2007). In *T. asahii*, the reduced negative charge is presumably an important parameter contributing to the lower efficacy of the trichosporal GXM to form aggregated gels during ultrafiltration of culture supernatants. In addition to influencing polysaccharide assembly, alterations in cell charge attributable to GXM may affect virulence, as suggested by Nosanchuk and Casadevall, (1997). Capsular enlargement in *C. neoformans* also depends on the size of polysaccharide fibers, given the linear correlation between GXM effective diameter and microscopic capsular size (Frasés et al., 2009). Therefore, the reduced negative charge of the *Trichosporon* polysaccharide and its reduced effective diameter may be related with the observation that, although both genera can synthesize GXM, only the polysaccharide components from *Cryptococcus* spp. form prominent India-ink visible capsules.

The structural similarities observed for the GXMs from *Cryptococcus* and *Trichosporon* may suggest similar functional aspects, including antigenicity, cell anchoring and influence on the interaction of the pathogens with host cells. In fact, a previous study demonstrated that an antibody raised against the cryptococcal polysaccharide reacts with the cell wall of *T. asahii* (Melcher et al., 1991). Our results confirmed that antibodies to cryptococcal GXM cross reacted with the *T. asahii* polysaccharide, which may be explained by the fact that both polysaccharides share common structural domains. Despite their similarities it is noteworthy that these polysaccharides appear to have very different structural functions in *Trichosporon* and *Cryptococcus* spp. The former genus does not have visible capsules and GXM appears to be a cell wall-associated polysaccharide that is also shed into culture media.

The *T. asahii* polysaccharide was detected in both cell-associated and extracellular fractions. Growth at 37 °C suggested that one of the *T. asahii* isolates down modulates GXM expression, raising questions as to whether the polysaccharide is relevant for *Trichosporon* during human or animal infections. Considering that GXM clearly works in favor of the fungus during infection of mammalian hosts by cryptococci (Monari et al., 2006), the variable ability of *T. asahii* to produce GXM under different conditions, including the host's temperature, may be related with its lower incidence as a human pathogen, in comparison with *C. neoformans*. This observation, however, contrasts with a previous study showing that production of extracellular GXM is increased after serial passage of *T. asahii* through mice (Karashima et al., 2002). Therefore, the possibility that the efficacy in GXM production is variable in different *Trichosporon* isolates cannot be ruled out. In addition, the lower detection of GXM by antibody-based tests in one of the *T. asahii* isolates could be a consequence of structural modifications that would result in altered serological properties, which could, in fact, represent a pathogenic strategy to escape the host defense.

GXM in *Trichosporon* species has been mainly characterized as a cell wall polymer (Ichikawa et al., 2001; Melcher et al., 1991). In this context, the similarities of cryptococcal and *Trichosporon* polysaccharides led us to evaluate if the connection of GXM with cell wall components would be similar in both genera. In *C. neoformans* and *C. gattii*, GXM anchoring to the cell wall was demonstrated to involve chitin-derived structures (Rodrigues et al., 2008a). These structures, which correspond to β 1,4-*N*-acetylglucosamine oligomers that are recognized by the lectin WGA, were demonstrated to form molecular ‘bridges’ connecting the cell wall with the capsule in non-dividing and, more frequently, budding cells. Chitin and chitin-related molecules accumulate in sites of yeast budding (Bulawa, 1993; Cabib et al., 2008). In this study, a relationship between yeast budding and WGA binding to capsule-associated structures was also suggested. Our current results suggested a similar profile of binding of the lectin to budding regions of *T. asahii*, which led us to evaluate whether cell wall chitin-derived oligomers would be involved in GXM anchoring in this species. In fact, chitinase treatment resulted in the release of wall-associated GXM to the extracellular space accompanied by a modified pattern of binding of mAb 18B7 to the fungal surface. Interestingly, chitinase treatment changed the localized profile of lectin binding to a diffuse profile. As suggested before in *C. neoformans* (Rodrigues et al., 2008a), this effect is probably a result of the generation of cell wall chitooligosaccharides after partial enzymatic hydrolysis of chitin. Considering that WGA interacts with β 1,4-*N*-acetylglucosamine oligomers, but not with chitin in its polymeric form (Rodrigues et al., 2008a), chitinase treatment would be expected to generate an increased number of cellular sites for lectin binding. Additional evidence that GXM anchoring to the cell wall is similar in the two species used in this study came from the fact that, as previously described for *C. neoformans* (Bryan et al., 2005), DMSO treatment extracted GXM from the cell surface of *T. asahii*. The ability of both *C. neoformans* and *T. asahii* to anchor GXM by similar molecular mechanisms suggests that other cell wall connectors, including the major structural polysaccharide α 1,3-glucan, are required for anchoring of the trichosporal polysaccharide, as clearly described for cryptococcal cells (Reese and Doering, 2003; Reese et al., 2007).

Phagocytosis studies demonstrated that, in comparison with *Candida* strains, *Cryptococcus* and *Trichosporon* isolates are more resistant to phagocytosis (Lyman and Walsh, 1994). Acapsular *C. neoformans* mutants are known to incorporate exogenously added GXM into their cell surface (Reese and Doering, 2003). Considering that the process of GXM anchoring to the cell wall in *C. neoformans* and *T. asahii* showed similar elements, we hypothesized that the *C. neoformans* mutant would be able to bind the heterologous GXM produced by *T. asahii*. In fact, Cap67 cells became coated with the *Trichosporon* GXM after incubation in culture supernatants. Besides indicating that the motifs required for cell wall connection of GXM in *C. neoformans* and *T. asahii* could be similar, this result allowed the design of experimental models to evaluate the antiphagocytic capacity of the *T. asahii* GXM. Our results demonstrated that coating with the *Trichosporon* GXM protects the *C. neoformans* acapsular mutant against phagocytosis by murine macrophages. To our knowledge, this is the first demonstration that GXM from non-*Cryptococcus* species is antiphagocytic.

In the cryptococcal model, antibodies to GXM modify the course of animal infections prolonging the survival of lethally infected mice (Casadevall et al., 1998). In addition, a monoclonal antibody to GXM is in clinical trial in humans (Larsen et al., 2005). In addition to being the target of therapeutic antibodies, the polysaccharide also represents a potential vaccine component that can elicit protective antibodies (Datta et al., 2008; Zhang et al., 1997). The similarities of the *Cryptococcus* and *Trichosporon* models described in this study suggest that antibodies raised against the cryptococcal polysaccharide could be therapeutic against *T. asahii* infections. The possibility that single therapeutic tools could be useful in different models of fungal infections highlights the importance of studies on the properties of GXM in *Trichosporon* species. In this context, detailed structural studies as those developed in the *Cryptococcus* model, as well as in vivo protection tests, are indispensable for validation of GXM as a therapeutic target in *Trichosporon* infections.

Acknowledgments

M.L.R. and L.N. are supported by grants from Coordenação de Aperfeiçoamento de Pessoal de Nível Superior (CAPES, Brazil), Conselho Nacional de Desenvolvimento Científico e Tecnológico (CNPq, Brazil), Fundação de Amparo a Pesquisa do Estado de São Paulo (FAPESP, Brazil) and Fundação de Amparo a Pesquisa do Estado do Rio de Janeiro (FAPERJ, Brazil). AC is supported by NIH Grants AI033142, AI033774, AI052733 and HL059842. Carbohydrate analyses were performed at the Complex Carbohydrate Research Center, University of Georgia (Atlanta), which is supported in part by the Department of Energy-funded (DE-FG-9-93ER-20097) Center for Plant and Microbial Complex Carbohydrates.

References

- Antachopoulos C, et al. Fungal infections in primary immunodeficiencies. *Eur. J. Pediatr.* 2007; 166:1099–1117. [PubMed: 17551753]
- Barbosa FM, et al. Glucuronoxylomannan-mediated interaction of *Cryptococcus neoformans* with human alveolar cells results in fungal internalization and host cell damage. *Microb. Infect.* 2006; 8:493–502.
- Bose I, et al. A yeast under cover: the capsule of *Cryptococcus neoformans*. *Eukaryot. Cell.* 2003; 2:655–663. [PubMed: 12912884]
- Bryan RA, et al. Radiological studies reveal radial differences in the architecture of the polysaccharide capsule of *Cryptococcus neoformans*. *Eukaryot. Cell.* 2005; 4:465–475. [PubMed: 15701808]
- Bulawa CE. Genetics and molecular biology of chitin synthesis in fungi. *Annu. Rev. Microbiol.* 1993; 47:505–534. [PubMed: 8257107]
- Cabib E, et al. Assembly of the yeast cell wall. Crh1p and Crh2p act as transglycosylases in vivo and in vitro. *J. Biol. Chem.* 2008; 283:29859–29872. [PubMed: 18694928]
- Casadevall A, et al. Characterization of a murine monoclonal antibody to *Cryptococcus neoformans* polysaccharide that is a candidate for human therapeutic studies. *Antimicrob. Agents Chemother.* 1998; 42:1437–1446. [PubMed: 9624491]
- Casadevall A, et al. Monoclonal antibody based ELISAs for cryptococcal polysaccharide. *J. Immunol. Methods.* 1992; 154:27–35. [PubMed: 1401941]
- Cherniak R, et al. *Cryptococcus neoformans* chemotyping by quantitative analysis of ¹H nuclear magnetic resonance spectra of glucuronoxylomannans with a computer-simulated artificial neural network. *Clin. Diagn. Lab. Immunol.* 1998; 5:146–159. [PubMed: 9521136]
- Datta K, et al. Therapeutic efficacy of a conjugate vaccine containing a peptide mimotope of cryptococcal capsular polysaccharide glucuronoxylomannan. *Clin. Vaccine Immunol.* 2008; 15:1176–1187. [PubMed: 18524882]
- Dubois M, et al. A colorimetric method for the determination of sugars. *Nature.* 1951; 168:167. [PubMed: 14875032]

- Feldmesser M, et al. Intracellular parasitism of macrophages by *Cryptococcus neoformans*. Trends Microbiol. 2001; 9:273–278. [PubMed: 11390242]
- Fenselau C, Johnson LP. Analysis of intact glucuronides by mass spectrometry and gas chromatography-mass spectrometry. A review. Drug Metab. Dispos. 1980; 8:274–283. [PubMed: 6105065]
- Frases S, et al. *Cryptococcus neoformans* capsular polysaccharide and exopolysaccharide fractions manifest physical, chemical, and antigenic differences. Eukaryot. Cell. 2008; 7:319–327. [PubMed: 18156290]
- Frases S, et al. Capsule of *Cryptococcus neoformans* grows by enlargement of polysaccharide molecules. Proc. Natl. Acad. Sci. USA. 2009; 106:1228–1233. [PubMed: 19164571]
- Ichikawa T, et al. Structural studies of a cell wall polysaccharide of *Trichosporon asahii* containing antigen II. Eur. J. Biochem. 2001; 268:5098–5106. [PubMed: 11589701]
- Karashima R, et al. Increased release of glucuronoxylomannan antigen and induced phenotypic changes in *Trichosporon asahii* by repeated passage in mice. J. Med. Microbiol. 2002; 51:423–432. [PubMed: 11990495]
- Kozel TR, Gotschlich EC. The capsule of *Cryptococcus neoformans* passively inhibits phagocytosis of the yeast by macrophages. J. Immunol. 1982; 129:1675–1680. [PubMed: 7050244]
- Larsen RA, et al. Phase I evaluation of the safety and pharmacokinetics of murine-derived anticryptococcal antibody 18B7 in subjects with treated cryptococcal meningitis. Antimicrob. Agents Chemother. 2005; 49:952–958. [PubMed: 15728888]
- Lyman CA, Walsh TJ. Phagocytosis of medically important yeasts by polymorphonuclear leukocytes. Infect. Immunol. 1994; 62:1489–1493. [PubMed: 8132358]
- McFadden DC, et al. The physical properties of the capsular polysaccharides from *Cryptococcus neoformans* suggest features for capsule construction. J. Biol. Chem. 2006; 281:1868–1875. [PubMed: 16278213]
- Melcher GP, et al. Demonstration of a cell wall antigen cross-reacting with cryptococcal polysaccharide in experimental disseminated trichosporonosis. J. Clin. Microbiol. 1991; 29:192–196. [PubMed: 1993757]
- Merkle RK, Poppe I. Carbohydrate composition analysis of glycoconjugates by gas-liquid chromatography/mass spectrometry. Methods Enzymol. 1994; 230:1–15. [PubMed: 8139491]
- Monari C, et al. Glucuronoxylomannan exhibits potent immunosuppressive properties. FEMS Yeast Res. 2006; 6:537–542. [PubMed: 16696649]
- Nimrichter L, et al. Self-aggregation of *Cryptococcus neoformans* capsular glucuronoxylomannan is dependent on divalent cations. Eukaryot. Cell. 2007; 6:1400–1410. [PubMed: 17573547]
- Nosanchuk JD, Casadevall A. Cellular charge of *Cryptococcus neoformans*: contributions from the capsular polysaccharide, melanin, and monoclonal antibody binding. Infect. Immunol. 1997; 65:1836–1841. [PubMed: 9125569]
- Panepinto J, et al. Sec6-dependent sorting of fungal extracellular exosomes and laccase of *Cryptococcus neoformans*. Mol. Microbiol. 2009; 71:1165–1176. [PubMed: 19210702]
- Pfaller MA, Diekema DJ. Rare and emerging opportunistic fungal pathogens: concern for resistance beyond *Candida albicans* and *Aspergillus fumigatus*. J. Clin. Microbiol. 2004; 42:4419–4431. [PubMed: 15472288]
- Reese AJ, Doering TL. Cell wall alpha-1,3-glucan is required to anchor the *Cryptococcus neoformans* capsule. Mol. Microbiol. 2003; 50:1401–1409. [PubMed: 14622425]
- Reese AJ, et al. Loss of cell wall alpha(1–3) glucan affects *Cryptococcus neoformans* from ultrastructure to virulence. Mol. Microbiol. 2007; 63:1385–1398. [PubMed: 17244196]
- Rodrigues ML, et al. Binding of the wheat germ lectin to *Cryptococcus neoformans* suggests an association of chitin-like structures with yeast budding and capsular glucuronoxylomannan. Eukaryot. Cell. 2008a; 7:602–609. [PubMed: 18039942]
- Rodrigues ML, et al. Extracellular vesicles produced by *Cryptococcus neoformans* contain protein components associated with virulence. Eukaryot. Cell. 2008b; 7:58–67. [PubMed: 18039940]
- Rodrigues ML, et al. Vesicular polysaccharide export in *Cryptococcus neoformans* is a eukaryotic solution to the problem of fungal trans-cell wall transport. Eukaryot. Cell. 2007; 6:48–59. [PubMed: 17114598]

- Vecchiarelli A. Fungal capsular polysaccharide and T-cell suppression: the hidden nature of poor immunogenicity. *Crit. Rev. Immunol.* 2007; 27:547–557. [PubMed: 18197800]
- Yoneda A, Doering TL. A eukaryotic capsular polysaccharide is synthesized intracellularly and secreted via exocytosis. *Mol. Biol. Cell.* 2006; 17:5131–5140. [PubMed: 17021252]
- Zaragoza O, et al. Capsule enlargement in *Cryptococcus neoformans* confers resistance to oxidative stress suggesting a mechanism for intracellular survival. *Cell. Microbiol.* 2008; 10:2043–2057. [PubMed: 18554313]
- Zaragoza O, et al. The polysaccharide capsule of the pathogenic fungus *Cryptococcus neoformans* enlarges by distal growth and is rearranged during budding. *Mol. Microbiol.* 2006; 59:67–83. [PubMed: 16359319]
- Zhang H, et al. Peptide epitopes recognized by a human anti-cryptococcal glucuronoxylomannan antibody. *Infect. Immunol.* 1997; 65:1158–1164. [PubMed: 9119446]

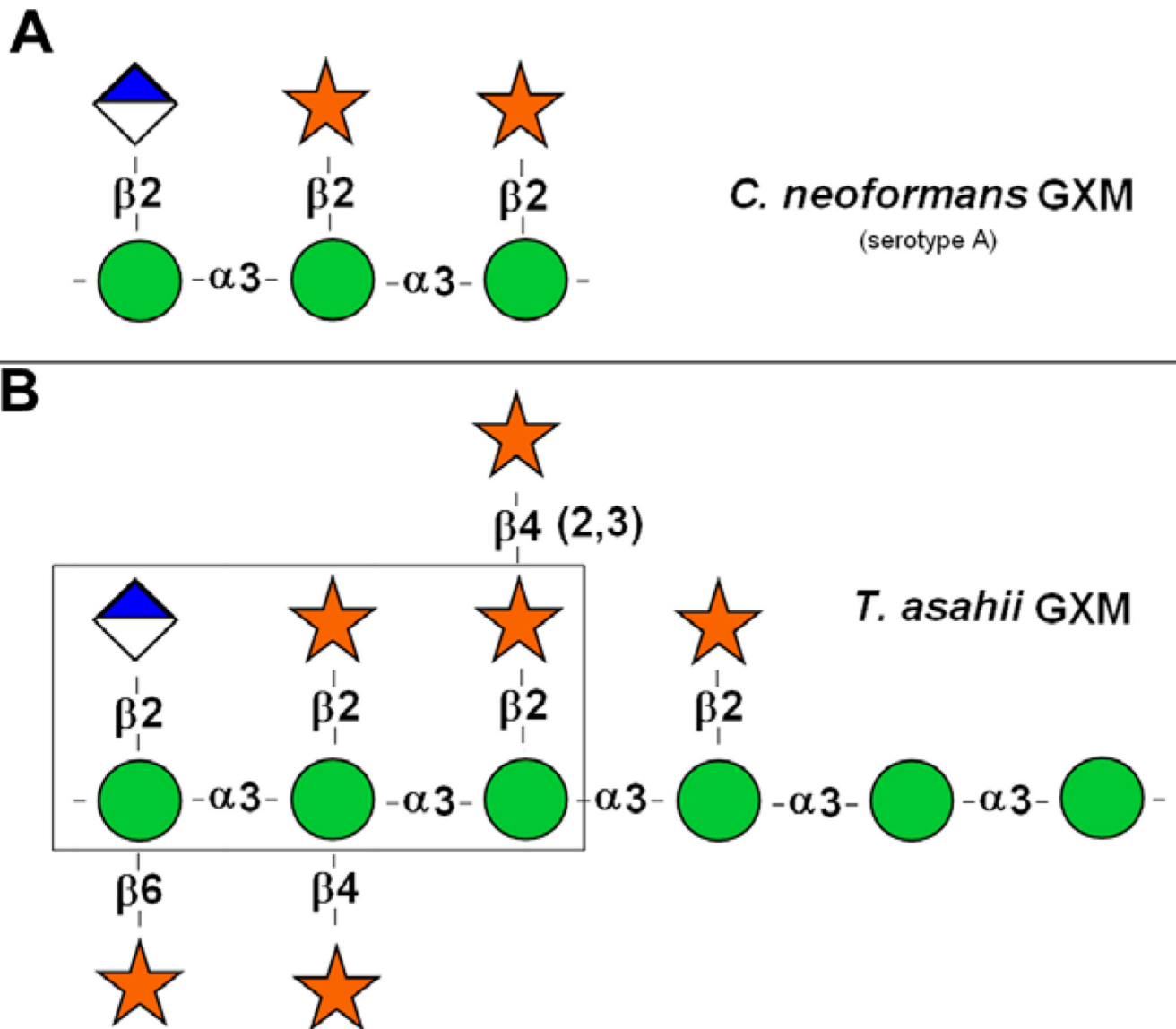


Fig. 1. Repeating motifs of *C. neoformans* (A) and *T. asahii* (B) GXMs. The boxed area in B is similar to the serotype A repeating motif of the cryptococcal GXM. Spheres represent mannosyl units; stars represent xylosyl units; diamond-shaped symbols represent glucuronyl units. Drawings of cryptococcal and *Trichosporon* GXMs were based on previous structural studies (Cherniak et al., 1998; Ichikawa et al., 2001). Structural differences include a higher variability in the type and positions of xylosyl substitutions for the trichosporal polysaccharide, which also shows a higher number of mannosyl units in its repeating motif.

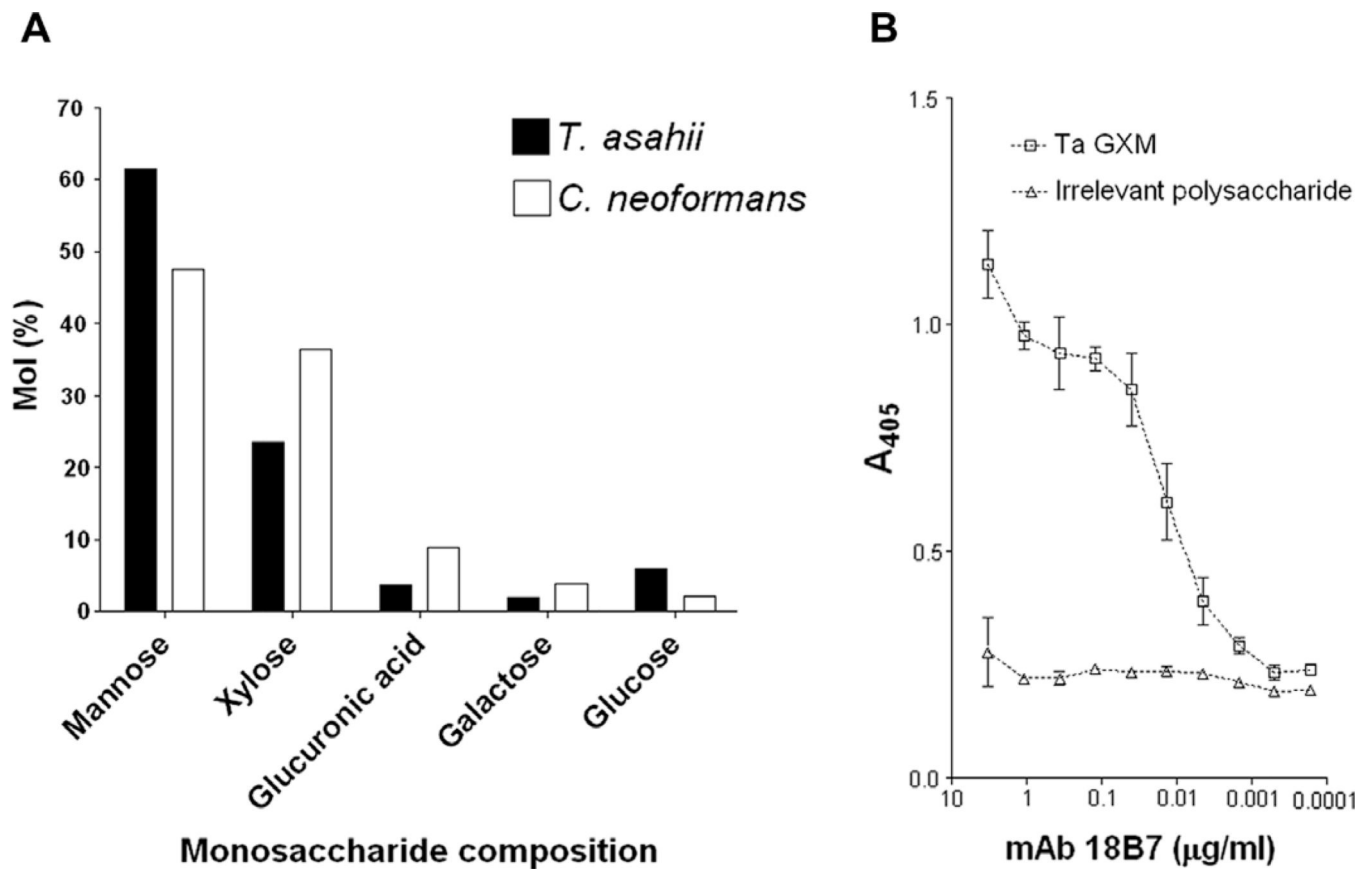


Fig. 2. Monosaccharide analysis and serologic properties of GXM fractions. (A) Monosaccharide composition of GXM fractions from *T. asahii* and *C. neoformans*, as determined by GC–MS. (B) Reactivity of the *T. asahii* GXM with a monoclonal antibody (mAb 18B7) raised against the cryptococcal polysaccharide. GXM is recognized by the antibody in a dose-dependent pattern. No significant reactions were observed when ELISA plates were coated with *S. cerevisiae* mannan (irrelevant polysaccharide). In all assays, ELISA plates were coated with 5 $\mu\text{g/ml}$ solutions of fungal polysaccharides.

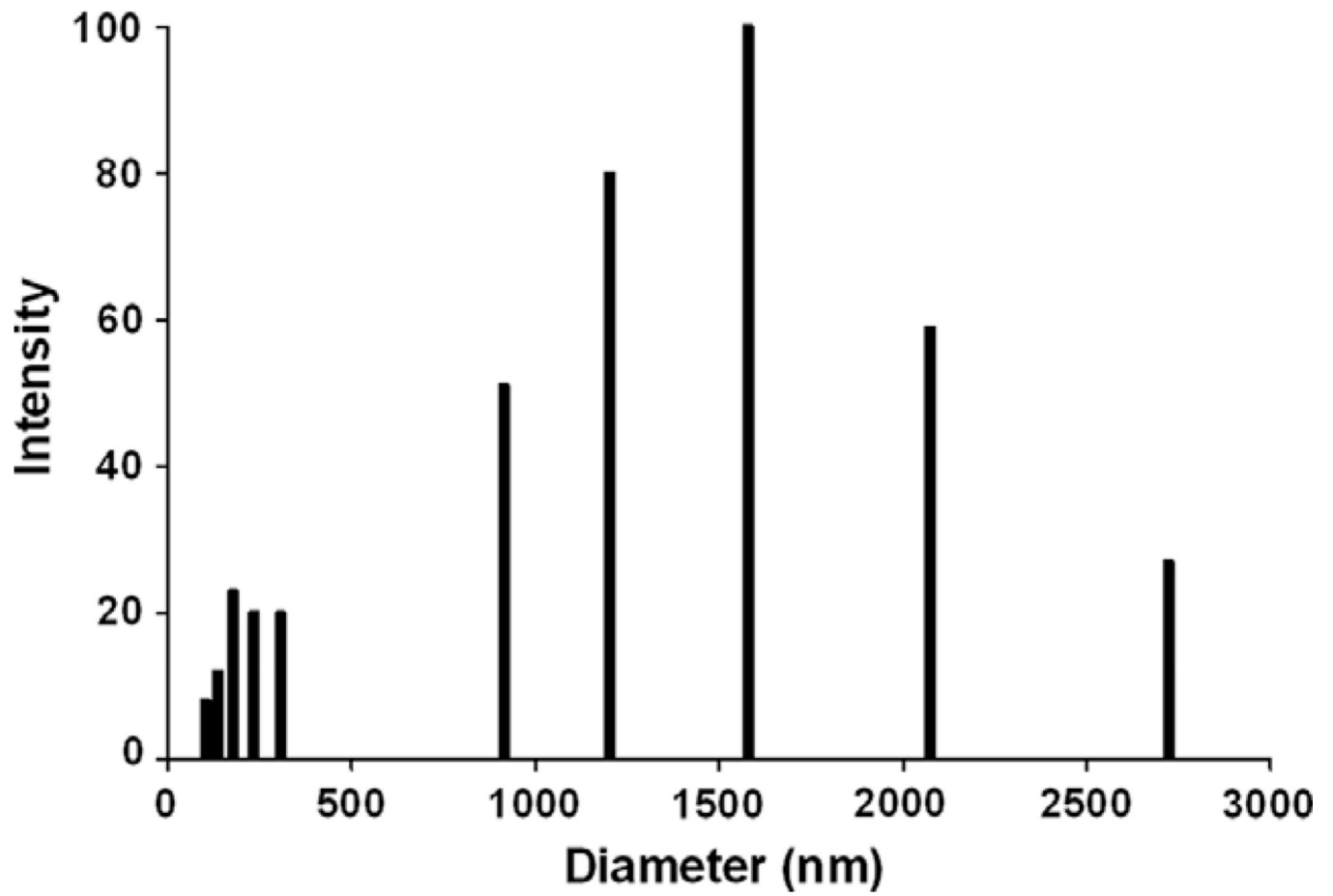
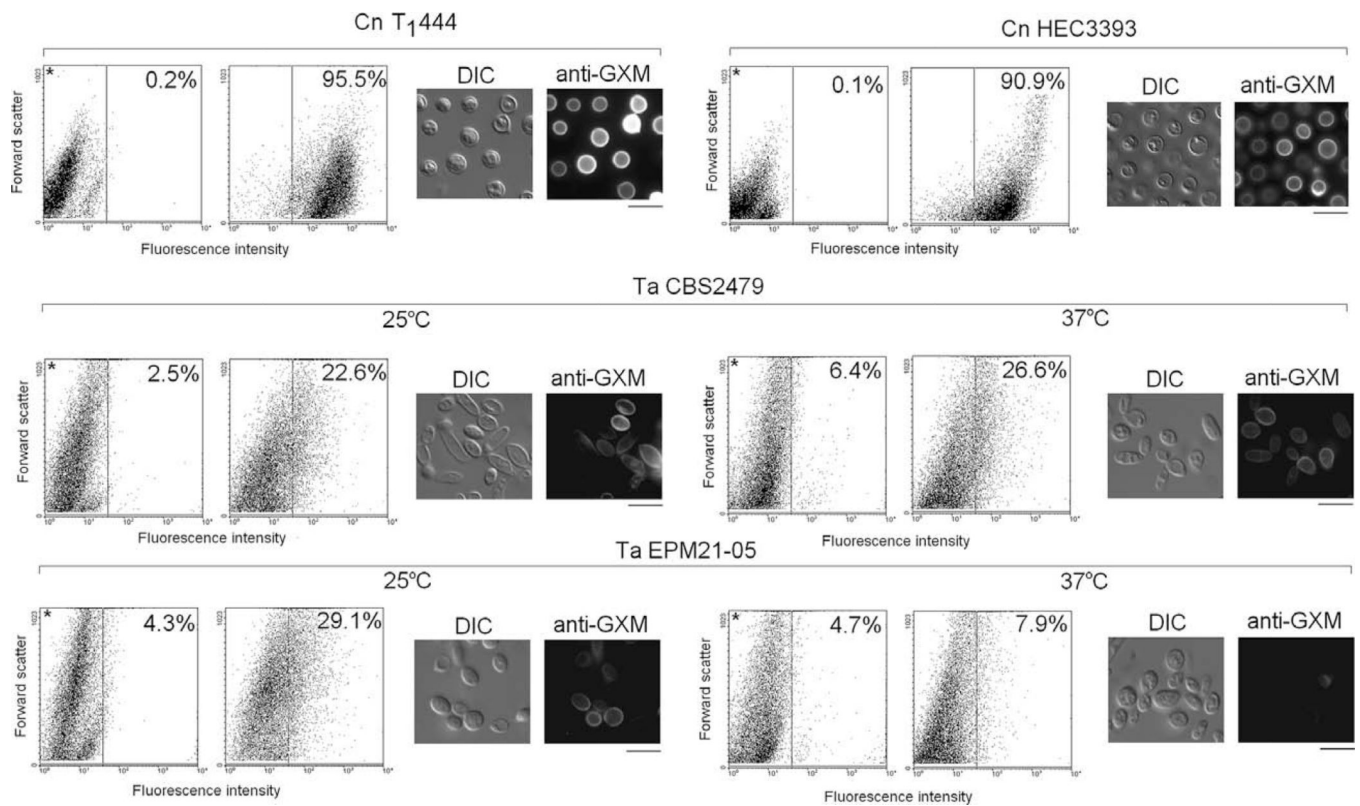


Fig. 3. Diameter distribution of GXM fibers isolated from *T. asahii*. An average value of 814.6 ± 35.3 nm was obtained.

**Fig. 4.**

Surface expression of GXM in *T. asahii* (Ta) and *C. neoformans* (Cn). Flow cytometry and fluorescence microscopy of fungal cells indicated that mAb 18B7 reacts with most of the *C. neoformans* cells, while the *T. asahii* population is only partially recognized by the antibody. The intensity of the fluorescent reactions with cryptococci is also higher. Polysaccharide expression by the Ta isolate EPM21-05 is apparently down modulated at 37 °C. In flow cytometry dot plots, asterisks denote control systems, in which fungal cells were not incubated with the anti-GXM antibody. The percentage of fluorescent cells is shown for each system. In fluorescence microscopy panels, fungal cells observed under differential interferential contrast (DIC) and fluorescence mode (anti-GXM) are shown. Scale bars, 5 μ m.

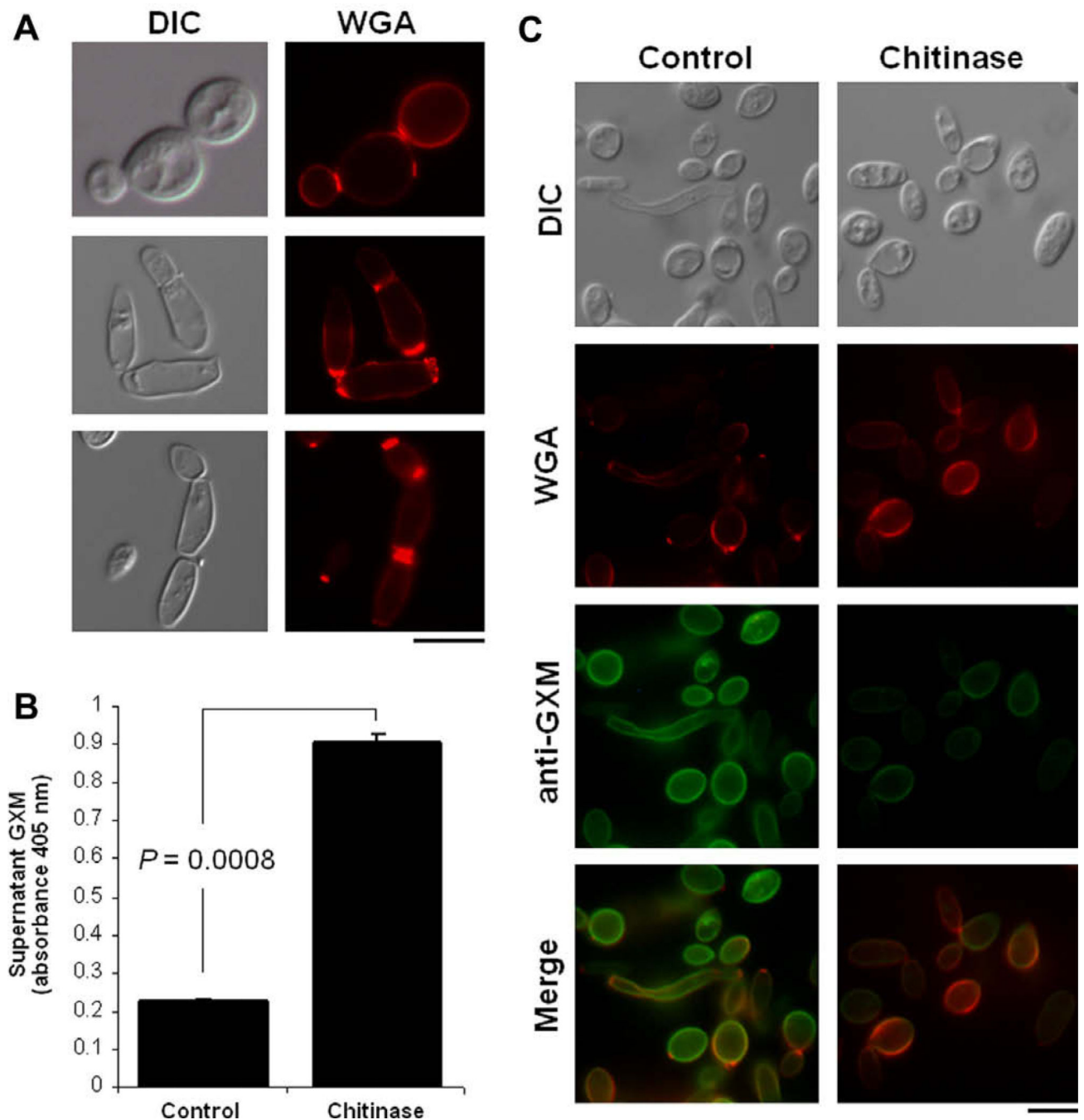


Fig. 5. GXM anchoring to the cell wall of *T. asahii* (isolate CBS2479) involves chitin oligomers. (A) Incubation of *T. asahii* cells with the lectin WGA reveals that external chitin-like structures are concentrated in cell division sites. Similar results of three different experiments prepared under the same conditions are shown. (B) ELISA of supernatants of *T. asahii* after incubation in PBS (control) or in the same buffer supplemented with chitinase reveals that GXM is released after exposure to the enzyme. (C) Incubation in the presence of the enzyme also changes the pattern of WGA binding to *T. asahii*. Analysis of the fungal

cells after the conditions described in B confirms the reduction in the content of surface GXM after chitinase treatment. Fungal cells observed under differential interferential contrast (DIC) and fluorescence mode (anti-GXM and WGA) are shown. Scale bars, 3 μm .

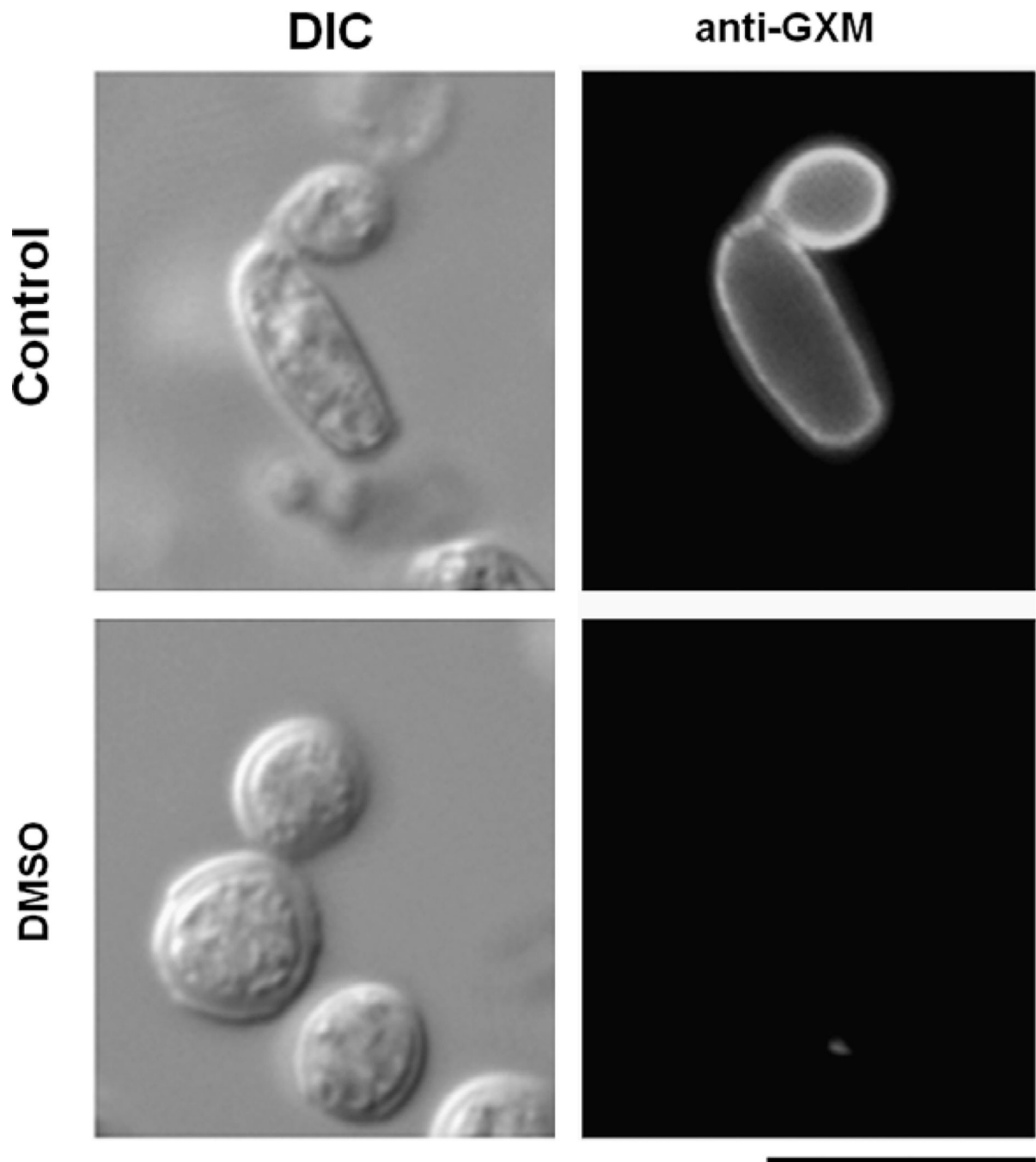


Fig. 6. Surface GXM is removed from the surface of *T. asahii* (isolate CBS2479) after treatment with DMSO. Fungal cells observed under differential interferential contrast (DIC) and fluorescence mode (anti-GXM) are shown. Scale bar, 3 μ m.

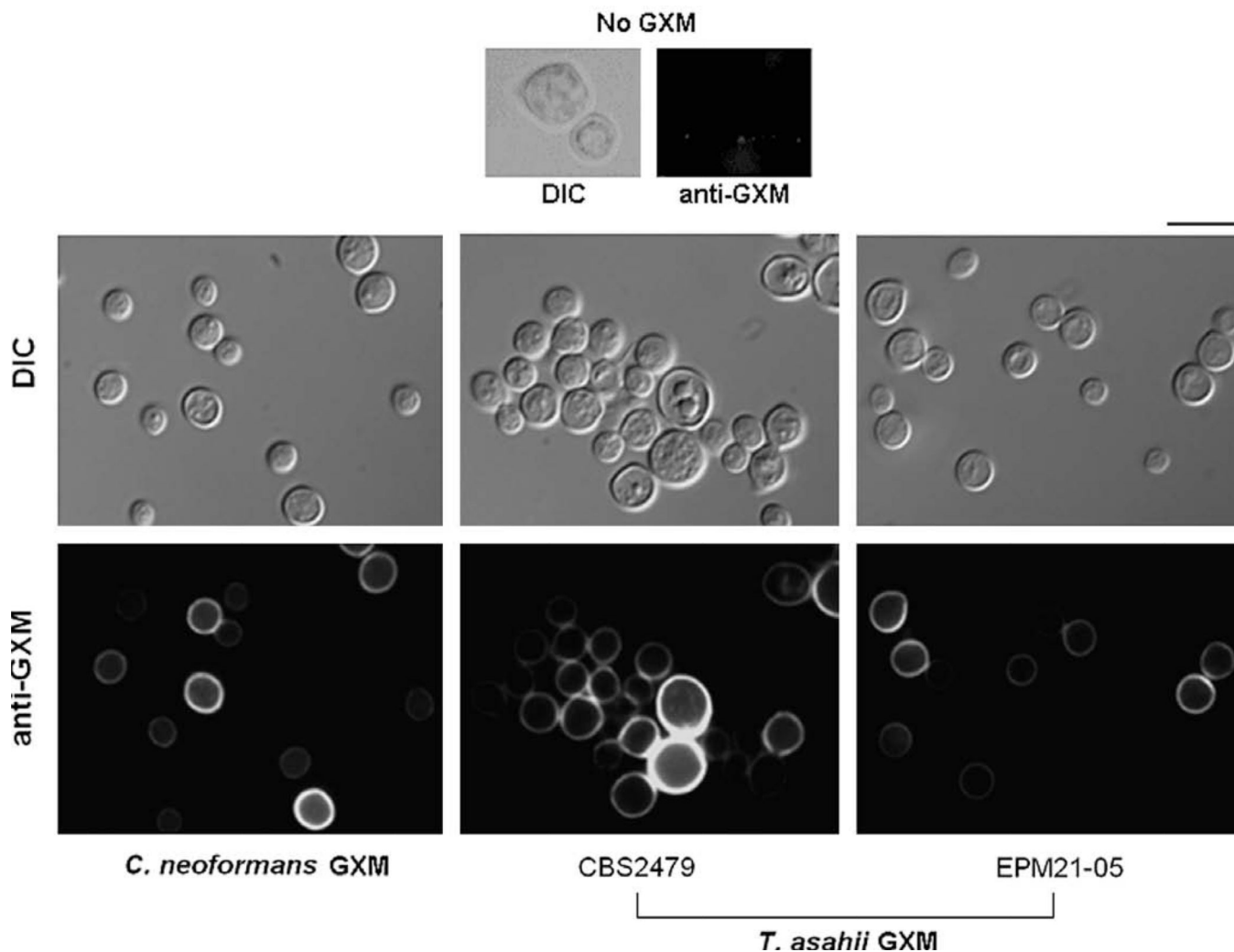


Fig. 7. Acapsular cells of *C. neoformans* incorporate GXM from culture supernatants of two *T. asahii* isolates. The culture supernatant of *C. neoformans* (strain T₁₄₄₄) was used as a positive control. Upper panels (No GXM) show immunofluorescence results after incubation of the acapsular mutant in sterile culture medium. Fungal cells observed under differential interferential contrast (DIC) and fluorescence mode (anti-GXM) are shown. Scale bar, 3 μ m. Images were acquired under identical conditions and processed similarly.

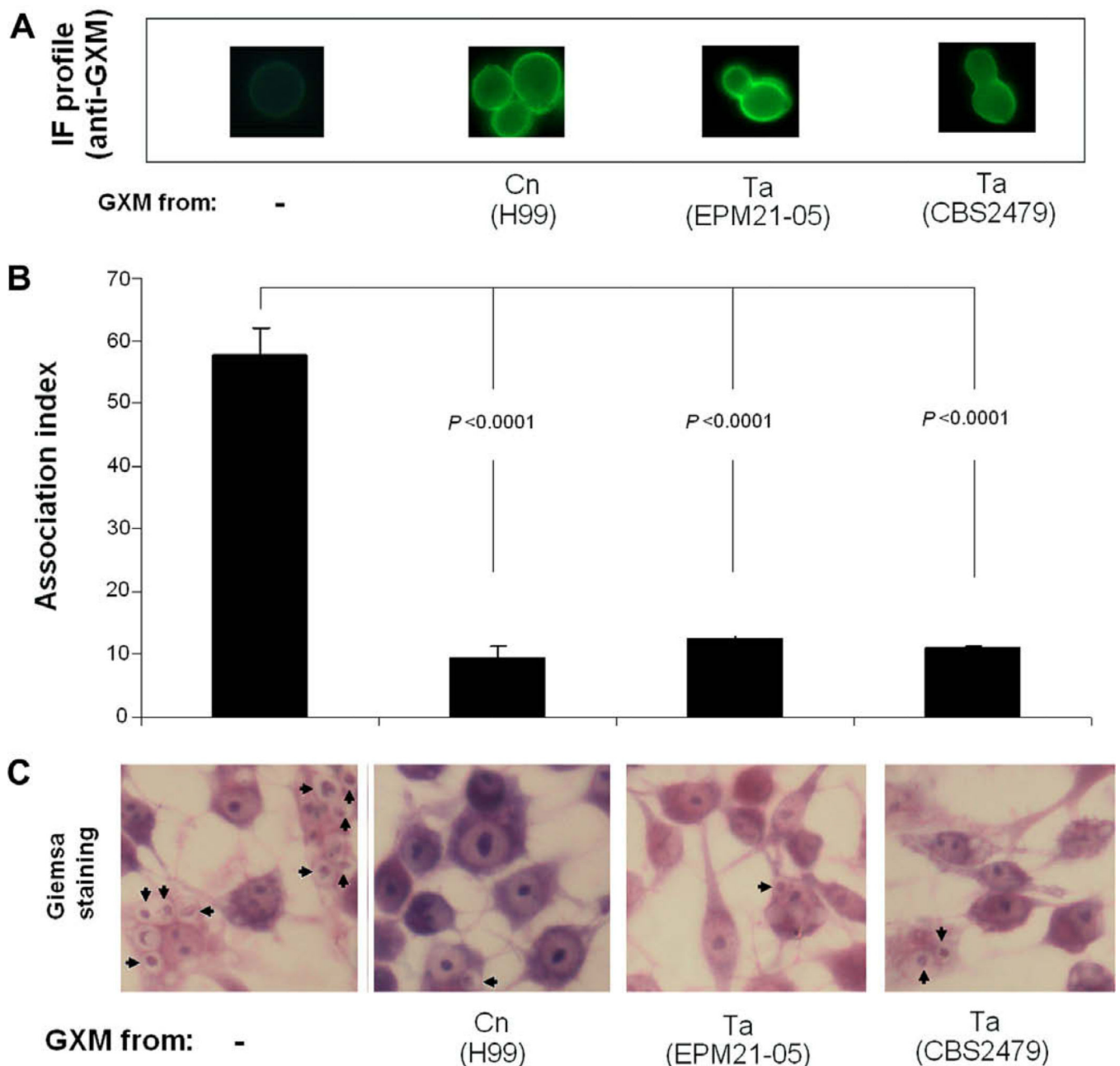


Fig. 8.

GXM from *T. asahii* supernatants turns acapsular mutants of *C. neoformans* more resistant to phagocytosis by mouse macrophages. (A) Cap67 cells were incubated in sterile medium (control, no GXM) or in the presence of culture supernatants of *C. neoformans* (Cn) or *T. asahii* (Ta). After polysaccharide incorporation, yeast cells were incubated with macrophages for determination of phagocytosis. (B) The number of phagocytes containing intracellular *C. neoformans* was significantly higher when yeast cells were not incubated in the presence of GXM. (C) Microscopy of Giemsa-stained, infected macrophages confirms

that GXM-coated cells are more resistant to phagocytosis. Arrows indicate intracellular Cap67 cells.

Table 1

Formation of GXM films after ultrafiltration of *T. asahii* and *C. neoformans* culture supernatants.

Pathogen	Culture volume ^a (ml)	Ratio of supernatant concentration ^a	Cell density ^a (cells/ml)	Gel volume ^b (ml)	Carbohydrate concentration in GXM films ^b (mg/ml)
<i>T. asahii</i>	6000	300-fold	2×10^7	0.5	0.9
<i>C. neoformans</i>	400	20-fold	7.5×10^7	1.0	11.9

^aMinimum values required for formation of GXM films.

^bValues obtained after supernatant concentration and formation of GXM films.